Wind Data Analysis, Annual Resource Estimation and Comparison with Measured Annual Energy Yield at the University Wind Turbine

James Maina Muriithi, Harrison Ngetha, Jean Byiringiro, Kevin Volkmer and Thomas Carolus

***Abstract*—Evaluation of the power potential of a particular type of wind turbine at a specific site is necessary for economic decisions. Therefore, the information of a wind turbine and that of a site have to be measured or predicted and then combined with the power curve of a wind turbine. The main objective of this research was to predict the power potential of the existing small wind turbine with a diameter of 3m and the wind turbine site at the University of Siegen and compare with the annual energy calculated from the measured one year of wind and turbine data. Techniques for prediction of the wind speed distribution of a site were determined and modeled. The power curve of the wind turbine was modeled from data recorded by applying a technique from the novel methods for modelling the power curve. In this research, artificial neural network, Weibull and Rayleigh are the techniques modeled to predict wind speed distribution at the wind turbine site. Rayleigh and Weibull were chosen since the two models depict a better wind speed distribution and require the mean and the standard deviation of the wind speed at the wind turbine site. A neural network trained with the backward propagation levernberg-Marquardt algorithm was applied to predict the wind speed and power potential of the wind turbine site. A comparison between Weibull, Rayleigh and the Levernberg-Marquardt trained neural network wind speed was made. The power curve of the wind turbine was successfully evaluated from wind data and wind turbine data recorded. The results indicate that the annual mean wind speed of the region is 2.54 (m/s) and about 20% of the wind availability was blowing from the west. The annual energy yield predicted from the trained neural network was 372 (kWh) closer to that determined from measured wind speed 360 (kWh) than that determined from Weibull and Rayleigh 337 and 233 (kWh) respectively. The three prediction models are applicable in any region to predict the annual energy of a particular wind turbine site with minimal data available.**

***Index Terms*—Rayleigh, Weibull, Artificial Neural Network, Power Curve, Annual Energy Prediction.**

I. Introduction

Renewable energy is defined as clean energy, environment-friendly energy source, inexhaustible; that is naturally replenished by sunlight, wind, rain, geothermal heat, and the waves [1]. Worldwide renewable energy has accorded 19.3% to the energy utilized by the whole of the wind turbine has decreased over the years and now is comparable to other renewable energy. The cost per MWh is competitive depending on turbine site selected [2].

To implement a wind turbine project in a given site, a thorough systematic analysis of wind distribution for a turbine site must be conducted [3]. The analysis of wind turbine site is achieved through the collection of wind data at the site or predicting the wind speed distribution and power at the site with minimal wind data or data provided from wind Atlas [3].

In the last decade, there is a tremendous increase in several types of research on techniques to predict wind speed distribution of a given region and power potential of a wind turbine site. The wind speed predictions techniques are classified into four main approaches: persistence, Artificial Neural Networks (ANN)/hybrids models and statistical techniques. The advantages of the artificial neural network over statistical technique are more precise and after training the network can be reused for prediction [4, 5]. The statistical techniques utilize mathematical models for analysis and evaluation of wind dataset. The statistical techniques in the same case as the ANN are based on time series data. The main advantages of statistical techniques over ANN are more straightforward, cost-effective and give a good representation of wind speed distributions [6, 7].

Various statistical techniques are applied to predict wind energy potential and to characterize the wind speed of a given wind turbine region [8]. In general, there are five primary statistical techniques Rayleigh distribution, Weibull distribution, lognormal distribution, Logistic distribution, and Gumbel distribution. Rayleigh and Weibull techniques are applicable where data is not recorded consistently or where the mean and standard deviation wind speed of the selected site is known [9].

To estimate the power potential of a site, the wind speed distribution measured or predicted is combined with the power curve of the wind turbine. A technique needs to be chosen and modeled to determine the curve. There are various methods applied to determine the power curve; the method of binning was applied to determine the power curve as recommended by [10].

Published on June 14, 2019.

J. M. Muriithi is with the Department of Mechatronic Engineering, Dedan Kimathi University of Technology, Private bag Nyeri, Kenya. (email: jemuse976@gmail.com)

H. T. Thuku is with Department of Electrical and Electronic Engineering, Dedan Kimathi University of Technology, Private Bag, Kenya; (email: harrison.ngetha@dkut.ac.ke)

J. Byiringiro is with the Department of Mechatronic Engineering, Dedan Kimathi University of Technology, Private bag Nyeri, Kenya. (email:jean.bosco@dkut.ac.ke)

T. Carolus is with the Institute of Fluid and Thermodynamic, Siegen University, Paul-Bonatz-Str 9-11, D-57076, Siegen, Germany; (email: thomas.carolus@uni-siegen.de)

K. Volkmer is with the Institute of Fluid and Thermodynamic, Siegen University, Paul-Bonatz-Str 9-11, D-57076, Siegen, Germany; (email:kevin.volkmer@uni-siegen.de)

II. Research at Small Wind Turbine Site of University of Siegen

A. *Experimental setup*

The existing wind turbine is a full-scale small horizontal axis wind turbine positioned on the rooftop of the Paul-Bonatz building of the University of Siegen, Germany as shown in Fig. 1. The wind turbine tower is 5 m above the roof and has a rotor diameter of 3m. It passively tracks wind through a wind vane: The rotor blades are self-designed at the University of Siegen with the design wind speed of 6.0 (m/s), design power of 400 W and a tip speed ratio of 7.5.

The asynchronous 3-phase alternating current (A.C) generator rated 2.5 kW was utilized to convert the torque generated by wind speed to electrical power.

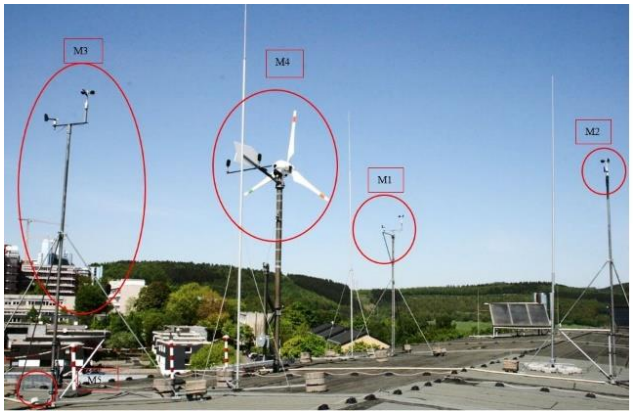

Fig. 1: wind turbine and Measurement stations M1, M2, M3 and M4 on the rooftop of the University of Siegen, Germany

B. *Measurement station arrangement at the turbine site*

The measurements stations are located three times the diameter of the rotor as recommended by [10] away from the center point of the wind turbine as illustrated in Fig. 2. The measurement stations one is located at 90^0.

The effective wind speed was determined by the average of wind speed acquired from three sensors, but if one of the three wind sensors was in the wake region, the signal from the measurement station in the wake region was not included as described in Fig. 2.

Data recorded for wind direction was assumed that the wake region has a small effect on the wind direction and therefore, the effective direction was achieved from the average of the three sensors [12].

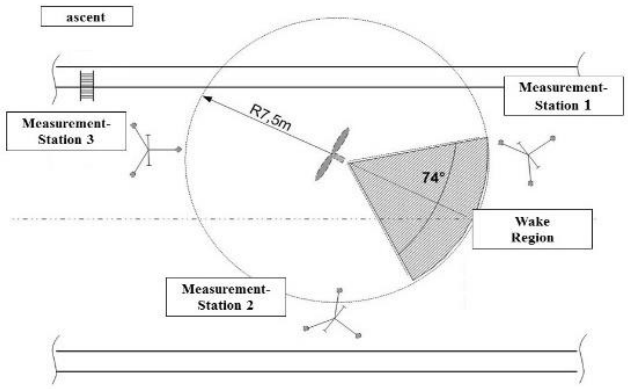

Fig. 2: A schematic top view measurement sensors arrangement and turbine at the wind turbine site [11].

C. *Experimental data processing*

The data was recorded as explained in Fig. 3, which gives an overview of how measurement data was recorded from the wind turbine site to the National Instruments (NI) measurements cards. The data acquisition was acquired continuously twenty-four hours per day and saved in the wind database. The parameters recorded are; Date and time, three wind speeds, three wind directions, The electrical power from the generator, the rotational speed of the rotor, temperature, humidity and air pressure. The data was transferred to the PC for processing and saving. The LabVIEW® software was installed in the PC contained subroutines programs known as Virtual Instruments (VI). The VIs subprogram gave commands for data saving in time series. Fig. 3 describes an overview of how data was recorded from the wind turbine and the environment.

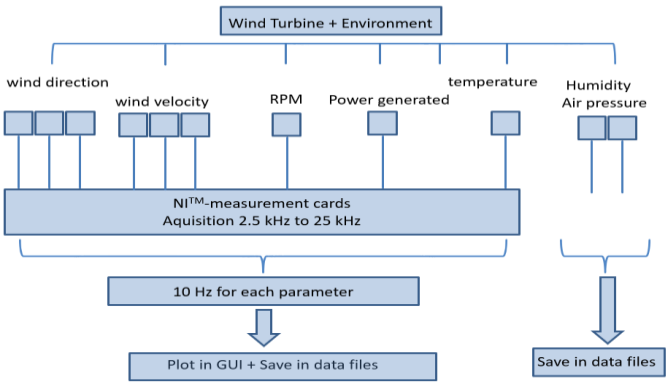

Fig. 3: Overview of data acquisition from the wind turbine and the surrounding via the NI measurement cards to the PC for processing and saving.

D. *Data conversion and evaluation*

Annually data recorded from 1st Jan–31st Dec 2017 was extracted from wind database. The data was saved with 10 Hz frequency that is one data point at every 0.1s, and each file contained 864000 data points. Wind direction, wind speed, power, time, air pressure, humidity, temperature and number of rotation of the rotor of wind turbine data points was applied in this research. The data was converted to Matlab files and averaged to one minute as recommended by [10] for a small wind turbine. Fig. 3 gives an overview of the data converted for the whole year.

The total time T when the wind speed data was recorded in hours was given as follows where N_i was the total number of data points for the whole year

$$T = \frac{N_i}{600} \tag{1}$$

TABLE I: Description Of Averaged Measured And Calculated Data Recorded From 1st Jan-31st Dec 2017

Names	Total number of data points	Unit
Wind speed	517,417	(m/s)
Wind direction	517,417	(°)
Electrical power	517,417	(W)
Temperature	517,417	(K)
Humidity	517,417	(g/m^3)
Air pressure	517,417	(bars)

E. Analyzing the distribution of wind direction at the small wind turbine site

When analyzing the wind density of a site, a windrose diagram was applied to show dominant wind direction as well as wind speed frequency. The procedure to create a wind rose using Matlab software was carried out as follows according to [13]

Step 1: The windrose diagram was divided into 12 sectors. The graphical circle has 360°. Therefore, each sector contains 30°.

Step 2: The 514,751 wind direction data points were applied to categorize the corresponding wind speed frequencies of occurrence in every sector.

Step 3: The categorized wind direction data was represented on the windrose circular graph as a line originating at the center of the circle. The magnitude of the line was scaled to the frequency calculated from the wind direction data. Equation (2) illustrates how each frequency f_i in every sector was determined in percentage frequencies. X_i represents the wind direction of data points of a sector i of the windrose graphical tool.

$$f_i = 100.\frac{X_i}{\sum_{i=1}^{12} X_i} \tag{2}$$

Step 4: The categorized wind direction data points in each sector were then grouped according to the wind speed range from 0 (m/s) wind speed to the maximum wind speed recorded. Each range of wind speed was assigned a particular code and represented in the windrose graphical tool.

F. Wind speed distribution

Rayleigh, Weibull distribution and artificial neural network are the statistical methods preferred in this study over the other methods to determine annual energy production [14] and [15]. The main advantage of Rayleigh and Weibull approaches shows wind speed distribution of a region where data was not recorded consistently and required knowledge of the mean wind speed of a given region [16]. Weibull distribution has two parameters, shape parameter k and scale parameter c and with knowledge of the mean wind speed and standard deviation [17] of a given site wind speed distribution can be predicted. Weibull and Rayleigh applied for wind data analysis and prediction of annual energy output.

1) Wind speed distribution of measured data

Wind speed distribution was presented using the binning method to categorize time series data measured for the annual year 2017 and to calculate annual energy Production (AEP). The 514,751 one-minute average yearly-recorded wind speed data points were categorized into wind speed intervals of 0.5 (m/s). Wind speed data were grouped into bins $N_t = 25$ of width $W_i = 0.5$ (m/s), bin positioned at w_i and f_i the frequency of occurrence at every bin. Wind speed data recorded are categorized into bins as illustrated by [9] refer to (3)

$$N = \sum_{i=1}^{N} f_i \tag{3}$$

The mean of wind speed $\bar{U}$ and the standard deviation σ_i was calculated as follows.

$$\overline{U} = \frac{1}{N}\sum_{i=1}^{N_t} m_i f_i \tag{4}$$

$$\sigma_i = \sqrt{\frac{1}{N-1}\left\{\sum_{i=1}^{N_t} f_i - N\left(\frac{1}{N}\sum_{i=1}^{N_t} m_i^2 f_i\right)^2\right\}} \tag{5}$$

2) Rayleigh model for wind speed distribution

Rayleigh distribution was applied to predict wind speed distribution of a given site and the available power of the wind of the small wind turbine at the University of Siegen. With the knowledge of mean wind speed calculated from the measured data. Rayleigh scale parameter c was taken as the mean wind speed. The value of the shape parameter k of Rayleigh distribution equals to two [15]. Equation (6) was modeled as follows by applying the mean wind speed calculated from the annual data.

$$p(U_0) = \frac{\pi}{2}\left(\frac{U_0}{\bar{U}^2}\right)e^{-\frac{\pi}{2}\left(\frac{U_0}{\bar{U}^2}\right)^2} \tag{6}$$

The frequencies of occurrence of wind speed were determined by applying the integral of the probability density function $p(U_o).U_{o,k}$ was the probability of wind speed $U_{o,k}$ positioned at k between wind speed $U_{0,x}$ and $U_{0,y}$.

The frequencies of occurrence of wind speed were determined by applying the integral of the probability density function $p(U_o).U_{o,k}$ was the probability of wind speed $U_{o,k}$ positioned at k between wind speed $U_{0,x}$ and $U_{0,y}$.

$$F(b) = P\left(U_{0,x} \le U_{0,k} \le U_{0,y}\right) = \int_{U_{0,x}}^{U_{0,y}} f(U_0)dU_0$$
$$\int_{U_{0,x}}^{U_{0,y}} f(U_0)dU_0 = \int_{U_{0,x}}^{U_{0,y}} \frac{\pi}{2}\frac{U}{\bar{U}}\exp\left(-\frac{\pi}{4}\frac{U}{\bar{U}}\right)^2 dU_0 \tag{7}$$

The cumulative distribution function was described in (7), and according to [18] the frequencies of occurrences of wind speed distribution can be estimated from two Rayleigh distribution by modelling the probability distribution equation into histogram based bins. References [19] and [3] suggests that the relative frequencies distribution of Rayleigh distribution can be predicted by the continuous shape of the Rayleigh distribution.

$$F(U_0)dU_0 = \int_{U_{0,x}}^{U_{0,y}} \frac{\pi}{2}\frac{U}{\bar{U}}\exp\left(\frac{\pi}{4}\frac{U}{\bar{U}}\right)^2 dU_0 \tag{8}$$

The Rayleigh distribution (6) $U_{0,y}$ was modeled into histogram from the integral and represented as follows $\Delta U_0 = U_{0,y} - U_{0,x}$ was the bin width centred at the position $U_{o,k}$. The mean wind speed $\bar{U}$ was applied in (4) to calculate the wind speed distribution of a given region.

$$\int_{U_{0,x}}^{U_{0,y}} f(U_0)dU_0 \cong p(U_{0,k})\Delta U_0 = \frac{\pi}{2}\left(\frac{U_0}{\bar{U}^2}\right)e^{-\frac{\pi}{2}\left(\frac{U_0}{\bar{U}^2}\right)^2} \quad (9)$$

Equation (9) was applied to obtain the time distribution of at the wind turbine site according to [9]. A Rayleigh modeled histogram was plotted by applying the product of (9), the change in wind speed at every bin and T was the overall period centred at bin position k. The Mean wind speed AMS was given from wind speed data set recorded from 1st Jan- 31st Dec the year 2017.

$$\Delta t_k(U_{0,k}) = \frac{\pi}{2}T\Delta U_0\left(\frac{U_0}{AMS^2}\right)e^{-\frac{\pi}{2}\left(\frac{U_0}{AMS^2}\right)^2} \quad (10)$$

3) Weibull distribution

Weibull distribution has two parameters. Scale factor c, and shape parameter k and are estimated from the annual mean speed AMS and standard deviation calculated from measured wind speed. The Weibull probability density function for wind speed distribution was given by (11) according to [20]

$$f(U) = \frac{k}{c}\left(\frac{U}{c}\right)^{k-1}e^{-\left(\frac{U}{c}\right)^k} \quad 0 \le U < \infty \quad (11)$$

To find the frequencies of occurrence of the wind speed in a given range (12) was applied. Weibull cumulative distribution function (CDF) was derived from the integral of the PDF (11). The Weibull CDF was applied to show that the probability of wind speed was less than or equal to given wind speed.

$$f(U) = \int_0^U \frac{k}{c}\left(\frac{U}{c}\right)^{k-1}e^{-\left(\frac{U}{c}\right)^k}dU \quad (12)$$

Equation (12) was modeled into a histogram for small integral and taking integral of a small range of U. The probability density function $f(U)$ evaluates the likelihood value of wind speed U occurring between a given range.

$$F(b) = P(U_{0,x} \le U_{0,k} \le U_{0,y})$$
$$\int_{U_{0,x}}^{U_{0,y}} f(U_0)dU = \int_{U_{0,x}}^{U_{0,y}} \frac{k}{c}\left(\frac{U}{c}\right)^{k-1}e^{-\left(\frac{U}{c}\right)^k}dU \quad (13)$$

Equation (13) was applied to create the Weibull model.

$$F(b) = \int_{U_{0,x}}^{U_{0,b}} \frac{k}{c}\left(\frac{U}{c}\right)^{k-1}e^{-\left(\frac{U}{c}\right)^k}dU \cong f(U_{0,k})\Delta U_0 \quad .(14)$$

TABLE II: THE VALUES OF k AND c WERE ESTIMATED AS FOLLOWS USING THE ANALYTICAL AND EMPIRICAL METHOD

Parameter	Empirical method	analytical method
Shape Parameter k	$\left(\frac{\sigma_U}{\bar{U}}\right)^{-1.086}$	$\left(\frac{\sigma_U}{\bar{U}}\right)^{-1.086}$
Scale Parameter c	$\frac{\bar{U}}{\Gamma\left(1+\frac{1}{k}\right)}$	$\bar{U}\left(0.568+\frac{0.433}{k}\right)^{\frac{1}{k}}$

A Weibull modeled histogram was derived by applying the product of the integral of (12), with bin width ΔU_o and T the overall period when data was recorded was centred at bin position n to represent wind distribution stepwise. $\Delta t(U_o)$ was the time duration of the bin, $\Delta U_{o,n}$ was the change in wind speed positioned at the bin n. The Weibull final model was described in (15);

$$\Delta t_n(U_{0,n}) = \Delta t_n T\frac{k}{c}\left(\frac{U}{c}\right)^{k-1}e^{\left(-\frac{U}{c}\right)^k} \quad (15)$$

4) Wind speed prediction by applying the artificial Neural network

To create the neural network to predict wind speed, the procedures were conducted as follows:

- Characterization of the wind data recorded.
- Created the network
- Configured the network
- Initialized the weights and the biases
- Finally trained the network
- Validated the network
- Re-used the trained neural network created to predict wind speed.

G. *The design of the Neural Network*

The design of the neural network was done using Matlab version 2018b. The neural network applied was the Nonlinear Autogressive with External (Exogenous) input (NARX) for predictions. The advantage of NARX was accurate as compared to Nonlinear Input-Output. NARX-has exogenous inputs that is the model can relate the current value of a time series to both, past values of the same series and current of the driving (exogenous) series. NARX was created with an error element that enabled the model not to predict not precisely the same value as the initial element applied during training.

In the design of a full artificial Neural Network, the three key components to put into consideration were the inputs, neurons, the hidden processing components/elements and the outputs of the neurons. To connect from one activity to precedent activity feed-forward connectors was applied.

There were two sets of weights each representing all the hidden layers' neurons activations and the governing of activations of output neuron. Fig. 4 shows the complete open-loop neural network with four inputs, 20 hidden layers and the output.

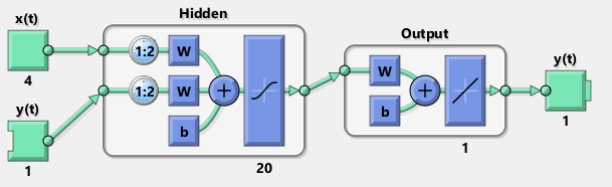

Fig. 4: The open neural network with four inputs wind direction, temperature, air pressure and humidity and target input as wind speed denoted by y (t).

Three types of learning algorithm were applied to train the neural network. The main three algorithm includes the Bayesian Regularization, scaled conjugate gradient and levenberg-Marquardt algorithm. The algorithm that gave the least MSE and the best regression was chosen for training. According to Table III Levenberg-Marquardt algorithm (LMA) depicted the least value of mean square error (MSE) and a regression much closer to 1 compared with the three algorithms. Therefore, LMA was chosen for training the created neural network.

TABLE III: RESULTS OF THE CHOSEN 3 TRAINING ALGORITHM TESTING WITH THE MSE AND REGRESSION RESPECTIVELY.

Name of the algorithm	MSE	Regression
Bayesian Regularization	2.29849e-2	9.97076e-1
Scaled conjugate gradient	2..6068e-2	9.96886e-1
Levenberg-Marquardt algorithm	2.37850e-2	9.97124e-1

The Levenberg Marquardt algorithm was applied to adjust the error between the target value and forecast wind speed. The adjustment begun from the output layer, vie each hidden layer to the antecedent hidden layer until the termination condition was achieved. The design of the neural network was summarized as follows;1

- Determination of the weights
- Normalizing inputs data
- Error propagation toward backward
- Termination conditions

During training, the network was trained with the four inputs data; wind direction, temperature, humidity and air pressure and the target value was the wind speed from recorded wind data at the wind turbine site. The error was minimized by varying the total hidden layers, the number of delays, learning parameters and the epochs applied for testing.

The Levenberg –Marquardt algorithm was distinctively devised to miniaturize the sum of square error as described by (16).

$$E = 1\frac{1}{2}\sum k\left(e_k\right)^2 = \frac{1}{2}\|e\|^2 \tag{16}$$

Where e_k was the error in the exemplar at k the position and e was the vector with element e_k.when the change between the antecedent and subsequent weight was small, the error vector was expanded by Taylor series first order derivative as shown in (17);

$$e_{(j+1)} = e_{(j)} + \partial e_k / \partial e_i \left(w_{(j+1)} - w_{(j)}\right) \tag{17}$$

Equation (17) error function was defined as follows;

$$E = \frac{1}{2}\left\|e_{(j)} + \partial e_k / \partial e_i \left(w_{(j+1)} - w_{(j)}\right)\right\|^2 \tag{18}$$

The error function was minimized with respect to the adjusted new vector weight as expressed in (17). In the Levenberg-Marquardt algorithm (LMA), the error function was adjusted by applying (18). Fig. 5 shows a fully trained closed neural network with four inputs and wind speed as the output target. The number of hidden layers applied was twenty and the number of delays chosen was two. The activation bias applied was the tansig function.

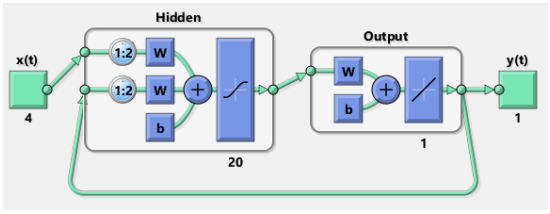

Fig. 5: The closed trained LMA neural network with four inputs wind direction, temperature, air pressure and humidity and y (t) the output Wind speed.

H. Power curve modelling of the small wind turbine

The modelling approach of the power curve of the wind turbine on the objective purpose, dataset available and desired accuracy [21]. To enhance maximum power generated from wind energy at a particular wind turbine site, it is essential to predict the expected power of a wind turbine. Therefore for any wind energy project, a precise estimation of power expected by a wind turbine at foreseeable future is of considerable significance [21]. Applying (19) the power generated P by a wind turbine as described by [22] and [23].

$$p = c_p \eta_m \eta_g \left[\frac{1}{2}\pi R^2 V^2\right] \tag{19}$$

The power produced by a wind turbine is directly proportional to the density of air ρ, wind speed u and turbine efficiency parameters $\left(c_p, \eta_m, \eta_g\right)$. The main advantage of the power curve was that it depicts the wind turbine characteristics without analyzing the technical aspects of turbine generator [23].

The measured power curve was evaluated from the power and wind data recorded using the method of binning as recommended by [10]. The power and wind speed data points were averaged in one-minute data. The power curve of a small wind turbine was determined as follows according to [10].

1) Step 1

The data points were normalised as recommended by [10] and wind and wind turbine data recorded when the wind turbine was not operating was discarded.

2) Step 2

The normalised, data sorted by applying the binning procedure, the height of the hub wind turbine was the same as that of the masts. A bin width of 0.5 (m/s) was applied in this approach to analyze the normalised wind speed data and normalised power output data set according to (20)

Normalised averaged wind speed in the bin i was given by v_i and the normalised wind speed of data set j in the bin i was denoted by $v_{n,i,j}$. The number of data points in the bin i was represented by $v_{n,i,j}$. In power measurement the normalised and averaged power output of data set j in the bin i as denoted as $P_{n,i,j}$ and the normalised and averaged power output at bin *i* was given by $P_{n,i,j}$.

$$v_i = \frac{1}{N_i}\sum_{j=1}^{N_i} v_{n,i,j}, P_i = \frac{1}{N_i}\sum_{j=1}^{N_i} v_{n,i,j} \quad (20)$$

I. Calculation of annual energy output

Calculated annual energy production was determined from the combination of power curve obtained and wind speed distribution calculated from measured data, Rayleigh and Weibull model. Measured annual energy production of the wind turbine was compared to Rayleigh predicted annual energy and Weibull predicted annual energy respectively. A comparison of the three methods was determined, and accuracy between Weibull and Rayleigh was evaluated to show which distribution with better estimate compared to measured annual energy.

The predicted wind speed in time series using the back propagation LMA neural network was multiplied with the power coefficient, area of the rotor of the small wind turbine and the calculated air density at the small wind turbine site to calculate the predicted power. A comparison between power predicted and that determined from measured wind speed was carried out. The annual energy output predicted was calculated by summing up the power predicted in (kWh).

III. Results and Discussions

A. Characterization of data at the wind turbine site

The wind rose diagram in Fig. 6 describes the wind characteristics at the turbine site for the yearly data of one minute averaged intervals. The total number of data points in each category data applied was 514,751 points.

The wind speed data was classified in a range of 2 (m/s) in every sector after categorizing the data points in the direction of the 30^0 range. The colour band describes the wind speed ranges. About 20 % frequency of wind speed was blowing from the west as described by the longest spoke. Less wind was expected from the North. Wind speed between 2 to 4 (m/s) was pre-dominant from any direction. The frequency of wind higher than 10 (m/s) was less than 5 %. Each concentric circle demonstrates a distinctive frequency, originating from the midpoint to increasing frequencies at the extrinsic circles.

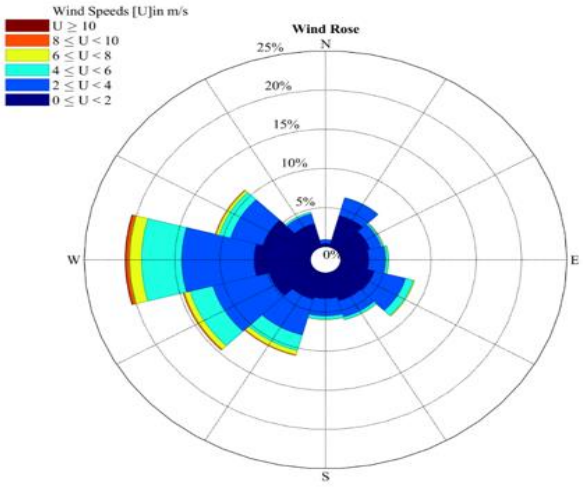

Fig. 6: Wind rose diagram characterizing wind speed and wind direction at the wind turbine site of the University of Siegen

B. Wind speed distribution

1) Measured and predicted wind speed distributions

Rayleigh prediction modeled indicating wind speed distribution at the site turbine was compared with the measured wind speed distribution. Fig. 7 describes the comparison between Rayleigh predicted annual wind speed distribution and measured annual wind speed grouped in 0.5 (m/s) bins and each bin centred at 0.25 (m/s). When the wind was below 2 (m/s) measured wind speed distribution is higher than the predicted Rayleigh modeled histogram time. At wind speed, higher than 2 (m/s) up to 4.5 (m/s) predicted wind speed time availability is higher than the measured wind speed. Also measured wind speed greater than 5 (m/s) depicts higher time availability compared to Rayleigh modeled histogram time.

Weibull predicted wind speed was compared with measured wind speed at the turbine site as described in Fig. 7. The Weibull distribution was closer to the measured wind speed. The predicted time availability for the Weibull model depicts a little deviation from the measured wind speed below 2.5 (m/s). The time availability for wind speed between 2.5 (m/s) to 5.0 (m/s) in the Weibull model much agreed with that of measured wind speed. There was a slight difference between measured wind speed for wind speed higher than 5.5 (m/s) to 9.5 (m/s). Wind speed greater than 10 (m/s) time availability in both cases time was less than 50 hours in the annual year.

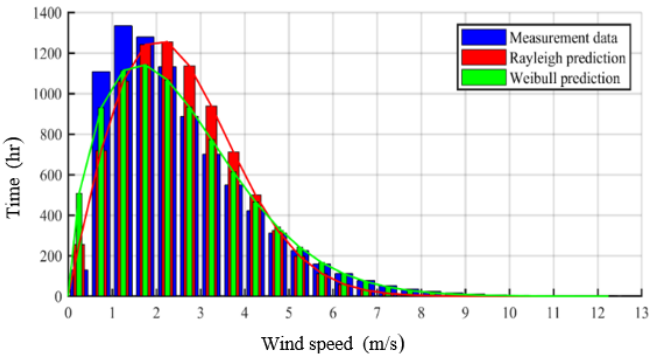

Fig. 7: Annual wind speed distribution of measured wind speed recorded and the predicted wind speed distribution from Rayleigh and Weibull models

2) Wind Speed prediction Using Artificial Neural network

The trained LMA neural network, validation and testing of the network output was described in Fig. 8. The error from the target and output during training, validation and testing was observed to be less than five when training, validation and testing of the network. This showed that the model was accurate and ready for reuse. Fig. 9 shows the error histogram with twenty bins during training, validation and testing of the model created. For all the instances, it can be observed that the data points were between -2.407 and 4.185. Fig. 9 shows that the model was well trained since the majority of data points are closer to zero error.

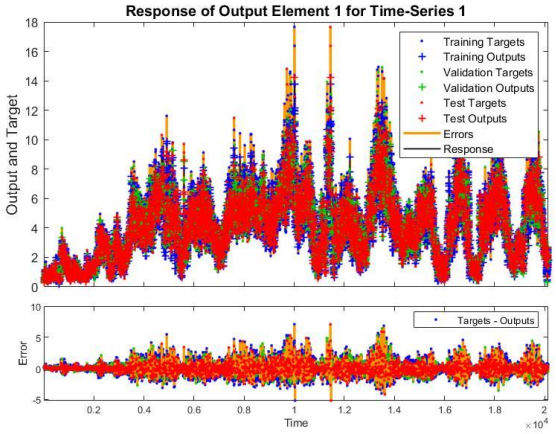

Fig. 8: The training, validation and testing of the neural network and the response after training the network

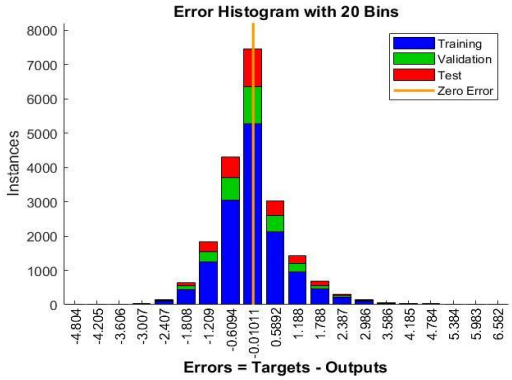

Fig. 9: Error histogram with 20 bins of the neural network model created

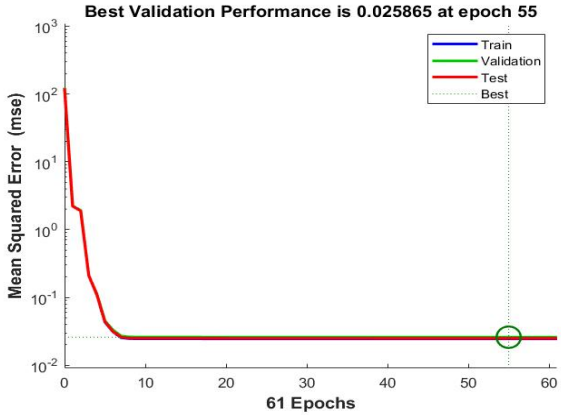

Fig. 10: Validation performance of the model during training, validation and testing.

Fig. 11 describes the best validation performance plot and it occurred at 55 epochs and the Means square error (MSE) was 0.025865, which was least during the simulation hence the model was well trained and was ready for re-use. The final mean-square error was small at 0.025865. From Fig. 10 it can be observed that test error and the validation set error displayed the same characteristics. There was no significant overfitting happen by iteration 56 and at this iteration, the perfect validation performance happened.

The performance analysis of the trained LMA network was carried out as described in Fig. 11. The regression r is 0.9908 and signifies an imminent relationship between the outputs and the inputs.

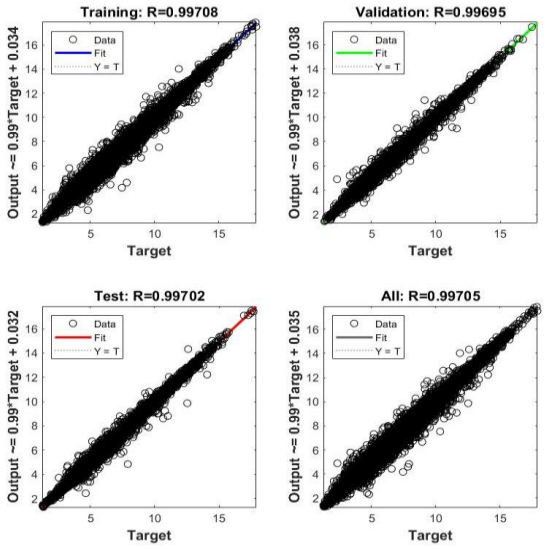

Fig. 11: Regression graph plots wind speed data during training, testing and validation of the LMA neural network model.

MRE was the mean squared difference between the outputs and targets. Lower values of MSE means the trained neural network is perfect. Regression R-values was 0.99705, which was a correlation between outputs and targets of the data points applied. An R-value of 0.99705 of the trained neural network means a close relationship hence the neural network was good since R was much closer to one.

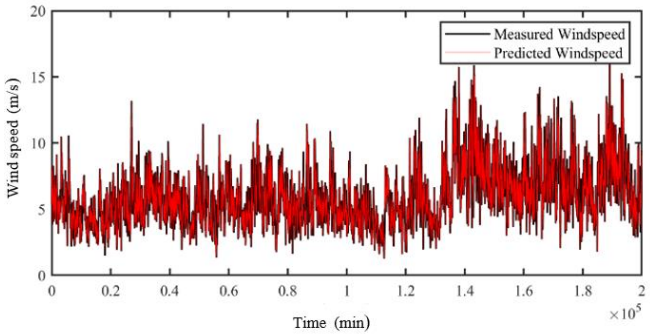

Fig. 12: The measured wind speed and the predicted wind speed in time series as predicted by the trained neural network.

C. Evaluation of the power curve of the small wind turbine at the University of Siegen

The measured power curve was obtained from the power-generated data and measured wind speed recorded. The measured power scatters plot was described in Fig. 13,

which illustrates the scatter plot of one minute averaged power data. At wind speed below 2 (m/s), there was no wind power data, and more power scatters data points are between 4 (m/s) and 8 (m/s). Some data points are observed above cut out wind speed, and power fluctuates as wind speed changes. At high wind speed, more data points are scattered on the upper part-indicating increase in power generated by the small wind turbine as wind speed increases.

The bar plot of Fig. 14 describes the average generated power in every bin. The power in every normalized bin increases with increases in wind speed. Generated power between wind speed 9 (m/s) and 12.5 (m/s) as described was almost constant since the turbine generator was operating at rated power range. When wind speed higher than 12.5 (m/s) the wind turbine the cut-out speed was reached hence the wind turbine turns to helicopter shifting the area of rotor away from incoming wind hence no power was generated.

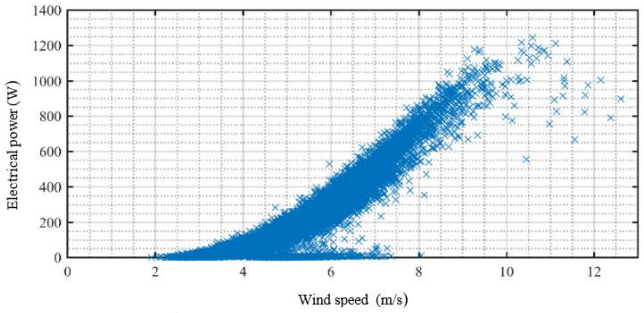

Fig. 13: Power performance scatters plot data one minute averaged data points.

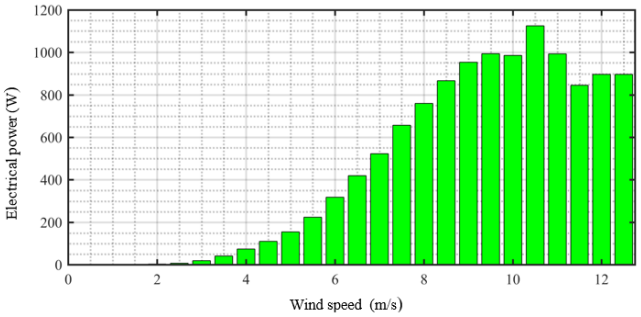

Fig. 14: Power bar plot illustrating the characteristics power curve of the generator of the small wind turbine at the University of Siegen, Germany.

D. Determining the Annual energy output

The annual energy distribution was calculated from the combination of the power bar plot obtained in Fig. 14 with the wind distribution calculated from the measured wind speed; Rayleigh predicted model and Weibull Predicted model. Fig. 15 describes the annual energy distribution (AED). Rayleigh predicted energy distribution showed a significant deviation change compared to the measured wind speed. Despite the changes in the estimation, the annual energy distribution values calculated between wind speed 2-5 (m/s) using the Rayleigh distribution model shows reasonable estimates and the results are closer to the measured. Rayleigh predicted AEP for wind speed between 5 (m/s) and 12 (m/s) displayed different values compared to measured data.

The Weibull predicted AED gave a reasonable estimate as wind speed varies the same as that of measured wind speed. For wind speed between 0-2 (m/s), annual energy outputs was zero as observed in Fig. 15. The energy predicted from both model shows a similar trend and energy harnessed around the design wind speed of the small wind turbine was 6 (m/s) is higher in the Weibull model than for Rayleigh. The energy increases higher around 5 (m/s) for the Weibull model while Rayleigh model energy predicted was high when wind speed was 4.5 (m/s)

Fig. 16 shows the comparison between the predicted power using the LMA backpropagation neural network and that determined from measured wind speed at the turbine site. From the plot, it can be observed that power generated was below 1000 Watts in most instances as time varies. Few instances where recorded whereby power was higher than the specified by generator above 1000 Watts this was because the torque produced by the wind was much higher than the recommended and the wind turbine was operating at its optimal point. Table IV gives total annual energy production (AEP) of calculated power from measured wind speed, LMA neural network prediction model, Rayleigh prediction and Weibull prediction respectively.

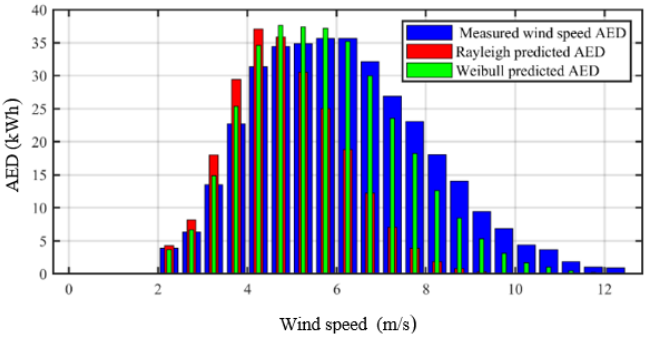

Fig. 15: Comparison of measured AED, Rayleigh predicted and Weibull predicted AED

The total energy was calculated for the prediction models and compared with that calculated from the measured data as shown in TABLE IV

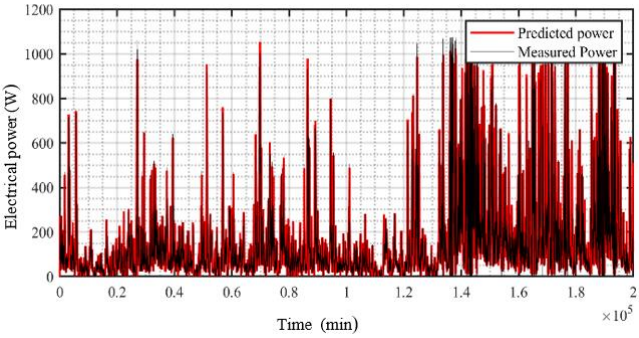

Fig. 16: Comparison of Predicted power applying the trained Neural network using LMA and power generated from the measured wind speed in time series.

TABLE IV: AEP FROM MEASURED WIND SPEED, RAYLEIGH, WEIBULL AND THAT DETERMINED BY TRAINED NEURAL NETWORK FOR THE YEAR 2017

Prediction technique	**AEP DETERMINED**
From measured wind speed	360.43 (kWh)
From Rayleigh model	233.39 (kWh)
Weibull model	337.15 (kWh)
Levenberg-Marquardt algorithm Neural Network	372 (kWh)

IV. Conclusions and Recommendations

From the research carried out, it was possible to predict the power potential of a particular site with knowledge of mean wind speed of a region by applying Rayleigh and Weibull model. The mean wind speed of the region was 2.54 (m/s) showing that the region is a low wind speed region. The wind speed distribution predicted using the LMA neural network depicted the same as that measured at the wind turbine site. At the turbine site, it was noted that 20 % of wind availability was blowing from the Western part. Annual energy production determined by the Weibull model was closer to that determined from measured wind speed. The wind power predicted using the trained neural network backward propagation LMA was closer to that determined from measured wind speed than that determined from the two statistical models. The annual predicted power by Weibull, Rayleigh and LMA neural network at the small wind turbine site was 233,337,372 (kWh) respectively. The annual power predicted by the LMA neural network was closer to that determined from measured wind speed.

This research has identified a possible further investigation that is, creating a model to predict the power potential of a site speed prediction by applying a hybrid technique of the statistical model incorporated in the LMA backpropagation neural network model.

Acknowledgment

Special thanks to the University of Siegen, Germany especially the Institute of Fluid and Thermodynamics for giving a chance to undertake this research at the Institute.

References

[1] N. L. Panwar, S. C. Kaushik, and S. Kothari, "Role of renewable energy sources in environmental protection: A review," Renewable and Sustainable Energy Reviews, vol. 15, no. 3, pp. 1513–1524, 2011.
[2] R. Gnatowska and E. Moryń-Kucharczyk, "Current status of wind energy policy in Poland," Renewable Energy, vol. 135, pp. 232–237, 2019.
[3] S. Mathew, "Analysis of wind regimes for energy estimation," Renewable Energy, vol. 25; Jg. 2002-03-01, no. 3, pp. 381–399, 2002.
[4] L. Mba, P. Meukam, and A. Kemajou, "Application of artificial neural network for predicting hourly indoor air temperature and relative humidity in modern building in humid region," Energy and Buildings, vol. 121, pp. 32–42, 2016.
[5] J. V. Tu, "Advantages and disadvantages of using artificial neural networks versus logistic regression for predicting medical outcomes," Journal of Clinical Epidemiology, vol. 49, no. 11, pp. 1996.
[6] S. K. Jha and J. Bilalovikj, "Short-term wind speed prediction at Bogdanci power plant in FYROM using an artificial neural network," International Journal of Sustainable Energy, vol. 2014, pp. 1–16, 2018.
[7] S. Makridakis, E. Spiliotis, and V. Assimakopoulos, "Statistical and Machine Learning forecasting methods: Concerns and ways forward." (eng), PloS one, vol. 13, no. 3, e0194889, 2018.
[8] B. Safari and J. Gasore, "A statistical investigation of wind characteristics and wind energy potential based on the Weibull and Rayleigh models in Rwanda," Renewable Energy, vol. 35, no. 12, pp. 2874–2880, 2010.
[9] J. F. Manwell, J. G. McGowan, and A. L. Rogers, Wind energy explained: Theory, design and application / J.F. Manwell and J.G. McGowan, Anthony Rogers, 2nd ed. Chichester: John Wiley, 2009.
[10] Power performance measurements of electricity producing wind turbines, 860, 2017.
[11] T. Gerhard, S. Michael, and T. Carolus, "Small Horizontal Axis Wind Turbine: Analytical blade design and comparison with a Rans-Prediction and First experimental data," Universität Siegen, 2013.
[12] K. Volkmer and T. Adam, "The wind Turbine of the University of Siegen," Institut für Fluid- und Thermodynamik, Feb. 2016.
[13] D. H. TDidane, N. Rosly, M. F. Zulkafli, and S. S. Shamsudin, "Evaluation of Wind Energy Potential as a Power Generation Source in Chad," International Journal of Rotating Machinery, vol. 2017, no. 1, pp. 1–10, 2017.
[14] M. Bassyouni et al., "Assessment and Analysis of Wind Power Resource Using Weibull Parameters," Energy Exploration & Exploitation, vol. 33, no. 1, pp. 105–122, 2015.
[15] F. A. L. Jowder, "Weibull and Rayleigh Distribution Functions of Wind Speeds in Kingdom of Bahrain," Wind Engineering, vol. 30, no. 5, pp. 439–445, 2006.
[16] A. David, "Rayleigh Distribution-Based Model for Prediction of Wind Energy Potential of Cameroon," Energy Review, vol. 1, no. 1, pp. 26–43, 2014.
[17] B. Hrafnkelsson, G. Oddsson, and R. Unnthorsson, "A Method for Estimating Annual Energy Production Using Monte Carlo Wind Speed Simulation," Energies, vol. 9, no. 4, p. 286, 2016.
[18] R. Gasch and J. Twele, Wind power plants: Fundamentals, design, construction and operation / [edited by] R. Gasch, J. Twele. Berlin: Solarpraxis; London : James & James, 2002.
[19] E. H. Lysen, "Introduction to Wind Energy: wind Energy development countries SWD," 1983.
[20] S. Nasiru, "Serial Weibull Rayleigh distribution: theory and application," IJCSM, vol. 7, no. 3, p. 239, 2016.
[21] I. Tizgui, F. El Guezar, H. Bouzahir, and B. Benaid, "Comparison of methods in estimating Weibull parameters for wind energy applications," Int J of Energy Sector Man, vol. 11, no. 4, pp. 650–663, 2017.
[22] S. Ashok, "Optimised model for community-based hybrid energy system," Renewable Energy, vol. 32, no. 7, pp. 1155–1164, 2007.
[23] A. Kusiak, H. Zheng, and Z. Song, "On-line monitoring of power curves," Renewable Energy, vol. 34, no. 6, pp. 1487–1493, 2009.